Isoform-specific differences in rapid nucleocytoplasmic shuttling cause distinct subcellular distributions of 14-3-3σ and 14-3-3ζ

Martijn J. van Hemert[1],*, Maarten Niemantsverdriet[2], Thomas Schmidt[3], Claude Backendorf[2] and Herman P. Spaink[1]

[1]Section Molecular Cell Biology, Institute of Biology, Leiden University, Wassenaarseweg 64, 2333 AL Leiden, The Netherlands
[2]Laboratory of Molecular Genetics, Leiden Institute of Chemistry, Leiden University, PO Box 9502, 2300 RA Leiden, The Netherlands
[3]Physics of Life Processes, Leiden Institute of Physics, Leiden University, Niels Bohrweg 2, 2333 CA Leiden, The Netherlands
*Author for correspondence (e-mail: hemert@rulbim.leidenuniv.nl)

Summary

Nucleocytoplasmic transport of proteins plays an important role in the regulation of many cellular processes. Differences in nucleocytoplasmic shuttling can provide a basis for isoform-specific biological functions for members of multigene families, like the 14-3-3 protein family. Many organisms contain multiple 14-3-3 isoforms, which play a role in numerous processes, including signalling, cell cycle control and apoptosis. It is still unclear whether these isoforms have specialised biological functions and whether this specialisation is based on isoform-specific ligand binding, expression regulation or specific localisation. Therefore, we studied the subcellular distribution of 14-3-3σ and 14-3-3ζ in vivo in various mammalian cell types using yellow fluorescent protein fusions and isoform-specific antibodies. 14-3-3σ was mainly localised in the cytoplasm and only low levels were present in the nucleus, whereas 14-3-3ζ was found at relatively higher levels in the nucleus. Fluorescence recovery after photobleaching (FRAP) experiments indicated that the 14-3-3 proteins rapidly shuttle in and out of the nucleus through active transport and that the distinct subcellular distributions of 14-3-3σ and 14-3-3ζ are caused by differences in nuclear export. 14-3-3σ had a $1.7\times$ higher nuclear export rate constant than 14-3-3ζ, while import rate constants were equal. The 14-3-3 proteins are exported from the nucleus at least in part by a Crm1-dependent, leptomycin B-sensitive mechanism. The differences in subcellular distribution of 14-3-3 that we found in this study are likely to reflect a molecular basis for isoform-specific biological specialisation.

Key words: 14-3-3 Proteins, 14-3-3 Localisation, Nucleocytoplasmic transport, Fluorescence recovery after photobleaching, FRAP

Introduction

The 14-3-3 proteins form a family of highly conserved acidic dimeric proteins, present in all eukaryotic organisms studied so far (for recent reviews, see Yaffe, 2002; Tzivion and Avruch, 2002; van Hemert et al., 2001). They are able to associate with over 100 binding partners and are involved in the regulation of a wide range of cellular processes, including signalling, cell cycle control, apoptosis, exocytosis, cytoskeletal rearrangements, transcription and enzyme activity.

Many organisms contain multiple isoforms – for example, in mammals nine isoforms have been identified (α, β, γ, δ, ε, ζ, η, τ and σ), but the reason for this variety remains unclear. It is not yet understood whether isoforms have distinct and specialised functions or whether they are just under the control of temporal and tissue specific regulation. Variations in temporal, developmental and tissue-specific isoform expression have indeed been reported (Yaffe, 2002; Leffers et al., 1993; Rittinger et al., 1999; Roth et al., 1994; Perego and Berruti, 1997; Tien et al., 1999). In addition, the expression of several plant and mammalian isoforms is influenced by external stimuli like temperature, injury and different types of stress (Yaffe, 2002; Jarillo et al., 1994; de Vetten and Ferl,

1995; Chen et al., 1994; Kidou et al., 1993). Besides differences in expression patterns, there are several reports on isoform-specific interactions with 14-3-3 binding partners (Yaffe, 2002; Wakui et al., 1997; Craparo et al., 1997; Meller et al., 1996; Liu et al., 1997; Van Der Hoeven et al., 2000; Tang et al., 1998; Peng et al., 1997; Zhang et al., 1997; Kumagai et al., 1998; Kurz et al., 2000; Hashiguchi et al., 2000). However, many functions can be performed by all 14-3-3 isoforms. Several binding partners, like Raf-1, BAD and Cbl, associate with all isoforms (Yaffe, 2002; Rittinger et al., 1999; Subramanian et al., 2001), and several 14-3-3-associating peptides have similar affinities for all isoforms (Muslin et al., 1996; Petosa et al., 1998). It is therefore likely that a combination of isoform-specific expression, localisation and functional specialisation is the basis for the existence of multiple isoforms.

In this report we focus on the human σ and ζ isoforms. 14-3-3ζ is abundant in various tissues and has been reported to interact with many of the known 14-3-3 ligands. 14-3-3σ (also called stratifin) is mainly expressed in epithelial cells (Leffers et al., 1993) and is strongly induced by ionising radiation and DNA damage through a p53-responsive promoter

element (Hermeking et al., 1997). In addition, it is involved in differentiation of keratinocyte stem cells (Pellegrini et al., 2001). 14-3-3σ appears to be involved in oncogenesis as it is downregulated in many breast cancers (reviewed by Yaffe, 2002) and hepatocellular carcinoma cells (Iwata et al., 2000), and it is overexpressed in several other cancers (Yaffe, 2002). 14-3-3σ acts as a tumour suppressor, inducing a G1 arrest by inhibiting Cdk2 and causing a G2 arrest by sequestering cyclin B1-cdc2 in the cytoplasm (Laronga et al., 2000; Chan et al., 1999; Hermeking et al., 1997). In contrast to 14-3-3ζ and other isoforms, 14-3-3σ does not bind to CDC25 (Peng et al., 1997).

Several 14-3-3 isoforms have been reported to be abundant in the cytoplasm and to be present in the nucleus of various organisms (Todd et al., 1998; Markiewicz et al., 1996; Fanger et al., 1998; Kumagai and Dunphy, 1999; Dalal et al., 1999; van Zeijl et al., 2000). 14-3-3s were also found to be associated with membranes (Martin et al., 1994; Roth et al., 1994; Jones et al., 1995; Tien et al., 1999), the cytoskeleton (Garcia et al., 1999; Ku et al., 1998; Roth and Burgoyne, 1995; Roth et al., 1994) and centrosomes (Pietromonaco et al., 1996). Some reports suggested a specific subcellular distribution for certain isoforms (Roth et al., 1994; Martin et al., 1994; Sehnke et al., 2000; Pietromonaco et al., 1996). However, a detailed comparison of isoform-specific localisation in one system has not been performed and all published studies are based on immunolocalisations in fixed cells. Here, we report on the isoform-specific and dynamic localisation of 14-3-3σ and 14-3-3ζ in living mammalian cells. We used yellow fluorescent protein (YFP) fusion constructs and showed that these were functional in vivo in yeast. We found that 14-3-3σ had a mainly diffuse cytoplasmic distribution in various mammalian cell types and that only low levels were present in the nucleus. By contrast, 14-3-3ζ was present at higher levels in the nucleus. We showed that both 14-3-3 proteins rapidly shuttle in and out of the nucleus, in part via a Crm1-mediated nuclear export mechanism. We performed fluorescence recovery after photobleaching (FRAP) experiments on living cells from which we conclude that a difference in nuclear export causes the different subcellular distributions of 14-3-3σ and 14-3-3ζ.

Materials and Methods
Strains, media and cell culture
The *Saccharomyces cerevisiae* strains used in this study were derived from GG1306 (*MATa leu2,3-112 ura3-52 trp1-92 his4 bmh1::LEU2 bmh2::APT1* Ycplac33[BMH2] (van Heusden et al., 1995)). Yeast strains were grown at 30°C in either MY or MYZ with 1% galactose (Zonneveld, 1986), supplemented as required with 30 µg/ml uracil, 20 µg/ml tryptophan, 20 µg/ml histidine and 1 mg/ml 5-fluoroorotic acid (5-FOA). Yeast was transformed according to the method of Gietz et al. (Gietz et al., 1995). NHK cells (normal human keratinocytes) were grown as described previously (Sark et al., 1998). Hela, HaCaT, NIH-3T3 and NHF cells (normal human fibroblasts, strain F9) were cultured in a 1:1 mixture of Dulbecco's modified Eagle's medium (DMEM) and Ham's F10, supplemented with 10% fetal bovine serum (Hyclone), streptomycin and penicillin.

Plasmids
The sequences of the oligonucleotides used in this study are listed in Table 1. Plasmids pMP4552 and pMP4558 encode 14-3-3σ and 14-3-3ζ, respectively, tagged C-terminally with YFP and under the control of the CMV promoter. pMP4552 and pMP4553 were constructed by cloning a fragment generated by PCR with primers P1 and P2 on a human keratinocyte cDNA library (Marenholz et al., 2001), followed by digestion with *Bam*HI, in pECFP-N1 and pEYFP-N1 (Clontech), respectively. A similar strategy was used to construct pMP4557 and pMP4558, which encode 14-3-3ζ, C-terminally tagged with CFP and YFP, respectively. For the latter constructs, a fragment generated by PCR with primers P3 and P4 on I.M.A.G.E. Consortium (LLNL) cDNA Clone 531246 (Lennon et al., 1996), followed by digestion with *Bam*HI, was used as insert. pYES-TRP[BMH2] allows the galactose inducible expression of *BMH2* (van Heusden et al., 1996). Yeast expression vector pMP4550, containing the *TRP1* marker and the *GAL1* promoter, was constructed by replacing the *URA3* gene of pYES2 (Invitrogen) with a 1.8 kb *TRP1* containing *Cla*I-*Bgl*I fragment from YEplac112 (Gietz and Sugino, 1988). Plasmid pMP4570 enables the galactose inducible expression of 14-3-3σ. This plasmid was made by inserting a synthetic DNA fragment consisting of oligonucleotides P5 and P6 in the *Hin*dIII-*Xba*I sites of pMP4550, followed by cloning a 0.8 kb 14-3-3σ containing *Sal*I-*Bsr*BI fragment from pMP4552 in the *Xho*I-*Sma*I sites of the resulting construct. Subsequently, a synthetic DNA fragment consisting of oligonucleotides P7 and P8 was cloned in the *Eco*RI-*Nar*I sites of this plasmid to improve expression. Plasmid pMP4585 enables the galactose inducible expression of 14-3-3ζ in yeast. A fragment containing 14-3-3ζ flanked by *Kpn*I and *Xba*I sites generated by PCR on pMP4558 with primers P9 and P10 was cloned in the *Kpn*I-*Xba*I sites of pMP4550. pMP4581 encodes a YFP and 6×His-tagged 14-3-3σ under control of the *GAL1* promoter and was constructed by cloning a 14-3-3σ-YFP-containing *Xma*I-*Not*I fragment from pMP4553 in pMP4571, after which a synthetic DNA fragment consisting of oligonucleotides P11 and P12 was inserted in the *Eco*RI-*Sma*I sites of this plasmid. pMP4583, which encodes 6×His-14-3-3ζ-YFP, was made in an analogous way, except that a 1.25 kb 14-3-3ζ-YFP-containing *Xma*I-*Not*I fragment from pMP4558 was used. Replacement of a 1.25 kb *Xma*I-*Not*I of pMP4583 with a 14-3-3ζ-CFP containing *Xma*I-*Not*I fragment from pMP4557 yielded

Table 1. Oligonucleotide sequences

P1	5′-CCGATGGATCCCATGGAGAGAGCCAGTCTGATC-3′
P2	5′-CTATGGATCCCGCCACCGCTCTGGGGCTCCTGGGGAG-3′
P3	5′-CGCGCGGATCCATGGATAAAAATGAGCTGGTTC-3′
P4	5′-CGCGGATCCCGCCACCATTTTCCCCTCCTTCTCCTG-3′
P5	5′-AGCTGAATTCCTCGAGATGAGAGGTTCTCATCACCATCACCATCACGGGGAATTCCCGGCTAGAAGCTTTAAGCGGCCGC-3′
P6	5′-CTAGGCGGCCGCTTAAAGCTTCTAGCCCGGGAATTCCCCGTGATGGTGATGGTGATGAGAACCTCTCATCTCGAGGAATTC-3′
P7	5′-AATTAATAAAAAAAATAATGGAGAGAGCCAGTCTGATCCAGAAGGCCAAGCTGGCAGAGCAGGCCGAACGCTATGAGGACATGGCAGCCTTCATGAAAGG-3′
P8	5′-CGCCTTTCATGAAGGCTGCCATGTCCTCATAGCGTTCGGCCTGCTCTGCCAGCTTGGCCTTCTGGATCAGACTGGCTCTCTCCATTATTTTTTTTATT-3′
P9	5′-GGGGTACCAAAAAATGGATAAAAATGAGCTGGTTC-3′
P10	5′-GCTCTAGATTAATTTTCCCCTCCTTCTCC-3′
P11	5′-AATTAGATCTAAAAATAATGCGAGGTTCTCATCACCATCACCATCACGG-3′
P12	5′-CCGTGATGGTGATGGTGATGAGAACCTCGCATTATTTTTAGATCT-3′
P13	5′-AGCTGAATTCCCGGGCTAGAAGCTTTAAGCGGCCGC-3′
P14	5′-CTAGGCGGCCGCTTAAAGCTTCTAGCCCGGGAATTC-3′

plasmid pMP4587. Plasmid pMP4584, which allows the expression of 6×His-14-3-3σ-CFP in yeast, was made by inserting a synthetic DNA fragment consisting of oligonucleotides P13 and P14 in the *Hin*dIII-*Xba*I sites of pMP4550, followed by cloning a 1.4 kb 14-3-3σ-CFP containing *Sfi*I-*Not*I fragment from pMP4552 in the *Sfi*I-*Not*I sites of the resulting plasmid.

Purification and analysis of recombinant 14-3-3 proteins

Yeast strains expressing various human 14-3-3 fusion proteins were grown in MYZ, 1% galactose, uracil, histidine to an OD_{620} of 0.5. All steps were performed at 4°C. Cells were lysed with glass beads in FastProtein Red tubes (Bio101) with a Fastprep FP120 (Bio101) in 50 mM Tris-HCl pH 8, 300 mM NaCl, 1% triton X-100, Mini Complete protease inhibitors, EDTA free (Roche) and 5 mM sodium-orthovanadate. Lysates were cleared by centrifugation and applied to a Ni^{2+}-NTA agarose (Qiagen) column. The column was washed with 50 mM Tris-HCl pH 8, 300 mM NaCl, followed by a gradient of 10-50 mM imidazole in the same buffer. Elution was done with 500 mM imidazole in 50 mM Tris-HCl pH 6.5, 300 mM NaCl. The eluted protein was dialysed twice against 500 volumes of 50% glycerol, 50 mM Tris-HCl pH 7.6, 300 mM NaCl, 1 mM DTT. Concentrations were determined by Bradford analysis and purity was estimated by SDS-PAGE followed by Coomassie staining. Gel filtration analysis of purified proteins was done with a 70 ml Sephacryl S200 column (Pharmacia) on a BioLogic system (Biorad), using molecular weight standards (Sigma) for calibration.

Cellular fractionation and western blot analysis

HaCaT cells were fractionated into nuclear extract and cytosol using the method of Brunet et al. (Brunet et al., 2002). Five micrograms of total protein from the cytosolic and nuclear extract were separated by 12% SDS-PAGE and proteins were transferred to PVDF by semi-dry blotting in 39 mM glycine, 48 mM Tris, 0.08% SDS, 20% methanol. 14-3-3σ and 14-3-3ζ were detected with specific antibodies (N-14 and C-16, respectively) from Santa Cruz Biotechnology. No cross-reactivity was found with these antibodies in a test with purified 14-3-3 proteins. Antibodies against actin (C-2), α-tubulin (B-7), PKCζ (C-20), RasGAP (B4F8) and p53 (DO-1) (Santa Cruz Biotechnology) were used in control experiments. All antibodies were diluted 1:1000. The BM Chemiluminescence Western Blotting Kit (Roche-Boehringer) was used for detection. Yeast protein extracts were subjected to immunoblotting as described above, except that Pan 14-3-3 antibodies were used to detect human 14-3-3 isoforms and anti-Bmh1p antiserum (van Heusden et al., 1995) was used to detect yeast 14-3-3 proteins. Antisera were diluted 1:5000.

Localisation of YFP-labelled 14-3-3 isoforms

Various mammalian cells were transfected with pMP4553, pMP4558 or pEYFP-N1 using DOTAP (N-[1-(2,3-dioleoyloxy)]-N,N,N-trimethylammoniumpropanemethylsulfate) (Roche). When desired, 20 ng/ml leptomycin B (LMB) was added to the medium 24 hours after transfection and cells were analysed at 0, 2, 4, 5 and 24 hours after addition with a Leica TCS NT confocal microscope. YFP was excited at 514 nm and emission was detected at 526-595 nm. Nuclear and cytoplasmic 14-3-3 levels were determined by quantifying the average YFP fluorescence of regions in the nucleus and cytoplasm of a z-section through the middle of the nucleus using the ImageJ program. The F_N/F_C ratio was calculated by dividing the nuclear value by the cytoplasmic value.

Immunofluorescence microscopy

HaCaT and Hela cells were grown on glass coverslips, fixed with methanol:acetic acid (3:1) and permeabilised with 50 mM Tris-HCl pH 7.4, 150 mM NaCl, 0.25% gelatine, 0.5% Triton X-100. Cells were stained overnight with specific anti-14-3-3σ (N-14) or anti-14-3-3ζ (C-16) antibodies (Santa Cruz Biotechnology), diluted 1:10. The primary antibody was omitted in control experiments. After washing three times, the coverslips were incubated three hours with Alexa-568 donkey anti-goat IgG (Molecular Probes) or Alexa-568 goat anti-rabbit IgG (Molecular Probes), diluted 1:50. After washing five times with PBS, cells were analysed with a Leica TCS NT confocal microscope. Alexa-568 was excited at 568 nm and emission was detected at 590-635 nm. Image analysis and quantification were done as described previously for YFP-labelled isoforms.
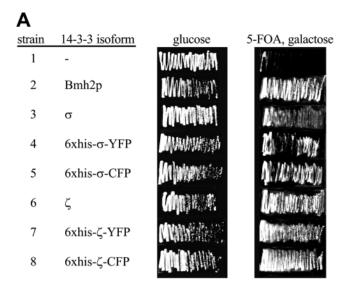
FRAP analysis

Fluorescence recovery after photobleaching (FRAP) experiments were done on a Leica TCS NT confocal microscope. YFP was excited at 514 nm at a laser power of 0.8 mW and emission was detected at 526-595 nm. After recording a pre-bleach image, a region covering >75% of the nucleus was photobleached by zooming in and scanning at high speed with maximum laser power (8 mW) for 3 seconds. Subsequently, images were captured at 1-second intervals during 2 minutes for YFP-labelled 14-3-3 proteins or at 4-second intervals during 8 minutes for YFP alone. During recording of the pre-bleach and time-lapse images, no significant photobleaching was observed for cells for which the photobleaching step was omitted. The change in nuclear fluorescence signal over time ($F_N(t)$) was quantified by image analysis with the LCS-NT software (Leica). $F_N(t)$ was normalised such that $F_N=0$ corresponds to the level of fluorescence immediately after photobleaching and $F_N=1$ corresponds to the final level of fluorescence at the end of the experiment. From the steady-state intensity distribution of nuclear (F_N) versus cytosolic fluorescence signal (F_C), the ratio of nuclear import (k_i) and nuclear export rate constant (k_e) was calculated using $k_i/k_e=F_N/F_C$. For analysis of the fluorescence recovery, we assumed that the nuclear volume was much smaller than the cytosolic volume, which means that F_C is constant and independent of the photobleaching process (actually we found that F_C decreased by <10%). Furthermore, it was assumed that photobleaching does not influence the import and export rates of 14-3-3. In this case exchange of photobleached molecules is governed by k_e and the process can be described by a first-order rate equation leading to a fluorescence recovery of $F_N(t)=1-e^{-k_e t}$. Data were fit to this equation leading to a value for k_e, and in combination with the steady-state distribution to the import rate constant $k_i=k_e \cdot F_N/F_C$. The half time ($\tau_{1/2}$), the time required to reach 50% recovery, was calculated using $\tau_{1/2}=\ln 2/k_e$. All calculations were based on measurements on at least 15 cells from two independent experiments.

Results

Recombinant YFP- and CFP-labelled human 14-3-3 proteins are functional in yeast

We set out to study the 14-3-3σ and 14-3-3ζ proteins in living human cells by making CFP and YFP fusion proteins. To test whether these are functional, we used a yeast-based assay. Disruption of the yeast 14-3-3 genes *BMH1* and *BMH2* is lethal and can be complemented by genes encoding 14-3-3 proteins from other organisms (van Heusden et al., 1995; van Heusden et al., 1996). Yeast strain GG1306 contains a *bmh1 bmh2* disruption, which is complemented by the *BMH2* gene on plasmid YCplac33[BMH2]. This strain was transformed with plasmids encoding wild-type and various recombinant 14-3-3σ or 14-3-3ζ isoforms under the control of the galactose-inducible *GAL1* promoter (Fig. 1A, left panel). The resulting strains were transferred to minimal medium containing
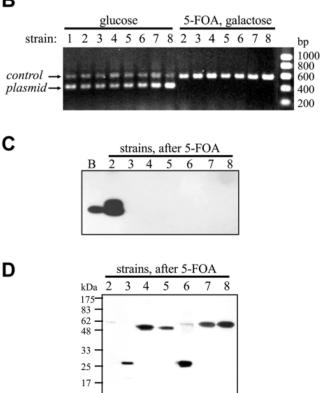
A

strain	14-3-3 isoform	glucose	5-FOA, galactose
1	-		
2	Bmh2p		
3	σ		
4	6xhis-σ-YFP		
5	6xhis-σ-CFP		
6	ζ		
7	6xhis-ζ-YFP		
8	6xhis-ζ-CFP		

B

C

D

Fig. 1. Recombinant human 14-3-3 proteins complement the lethal disruption of yeast 14-3-3 genes. (A) GG1306-derived yeast strains expressing the indicated 14-3-3 isoforms were transferred from glucose medium (left) to 5-FOA-containing medium (right). Strains can only grow on this medium when they are able to lose plasmid YCplac33[BMH2], illustrating the ability of the foreign 14-3-3 isoform to take over the function of the yeast 14-3-3 proteins. (B) The absence of plasmid Ycplac33[BMH2] after 5-FOA treatment was determined by PCR. This plasmid yields a 400 bp product, besides a 600 bp internal control product. Western blots on 5 μg (C) or 2.5 μg (D) total protein from strains after 5-FOA treatment with an antiserum against yeast 14-3-3 proteins (C) or against *Pan* 14-3-3 proteins (D). Lane b contains 20 ng purified Bmh2p.

galactose, 5-FOA, uracil and histidine, on which they can only grow when they are able to lose plasmid YCplac33[BMH2]. Strains expressing human 6×His-14-3-3ζ-CFP or 6×His-14-3-3ζ-YFP grow as good as cells expressing the yeast Bmh2p protein (Fig. 1A, right panel), indicating that these 14-3-3 isoforms can complement the *bmh1 bmh2* disruption. Human 14-3-3σ constructs also complement, although strains expressing these proteins grow slower compared with strains expressing Bmh2p or 14-3-3ζ. A strain carrying the empty vector (Fig. 1A, strain 1) was not able to grow on 5-FOA containing medium.

To rule out the possibility that mutations in the *URA3* gene of plasmid Ycplac33[BMH2] enabled strains to grow on medium with 5-FOA, we checked for the absence of plasmid Ycplac33[BMH2] by PCR. A 400 bp product is formed with plasmid Ycplac33[BMH2] as template and a 600 bp internal control product is formed with the genomic *bmh2* locus as template. Before 5-FOA treatment, both products were obtained (Fig. 1B, glucose). After 5-FOA treatment the 400 bp product was absent, while the 600 kb control product was still present (Fig. 1B), indicating the absence of Ycplac33[BMH2].

In addition, the absence of the yeast 14-3-3 proteins in strains growing on 5-FOA was shown by western blotting with an antibody against Bmh1p and Bmh2p (Fig. 1C). The clear band present in a strain expressing Bmh2p (Fig. 1C, strain 2) is absent in the strains expressing human isoforms. The presence and expression level of recombinant human 14-3-3 isoforms was investigated by western blotting with a Pan 14-3-3 antiserum. The yeast Bmh2 protein was not recognised by this antiserum (Fig. 1D, lane 2). The mobility of 14-3-3σ, 14-3-3ζ and the 6×His-tagged CFP and YFP fusion proteins was in agreement with their predicted mass (Fig. 1D, lane 3-8). 14-3-3σ constructs had slightly lower expression levels compared with 14-3-3ζ constructs, which might explain the slower growth of strains complemented by 14-3-3σ. Expression levels of the recombinant 14-3-3s were estimated to be 1-2% of total protein.

These results show that solely the human recombinant 14-3-3 isoforms are responsible for the complementation of the lethal *bmh1 bmh2* disruption in yeast cells. Our data indicate that human recombinant 14-3-3 proteins are functional in yeast and that an N-terminal 6×His-tag and a C-terminal CFP or YFP fusion do not interfere with at least the essential 14-3-3 function(s).

6×His-14-3-3σ-CFP forms dimers and associates with a Raf-1-based peptide

6×His-tagged CFP and YFP fusions of 14-3-3σ and 14-3-3ζ were purified from yeast to a purity of more than 95%. The proteins had a molecular mass of ~57 kDa in SDS-PAGE (Fig. 2A), which corresponds to the predicted molecular mass of a monomer. Gelfiltration of purified 6×His-14-3-3σ-CFP yielded an elution profile with a single peak corresponding to a mass of 116 kDa (Fig. 2B). This indicates that the protein forms dimers and that dimerisation is not affected by the introduction of an N-terminal 6×His-tag near the dimerisation domain. For the other 14-3-3 fusion proteins similar results were obtained (data not shown).

Both 14-3-3σ-YFP and 14-3-3ζ-YFP bound a Raf-1-based peptide with similar affinity as the yeast 14-3-3
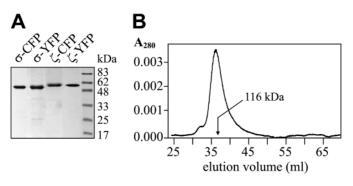
Fig. 2. Recombinant human 14-3-3 isoforms form dimers. (A) Coomassie-stained polyacryl-amide gel of recombinant human 14-3-3 isoforms purified from yeast. (B) Gel filtration analysis of 6×his-14-3-3σ-CFP.

protein Bmh2p in fluorescence correlation spectroscopy measurements (R. Schmauder, unpublished). This suggests that the C-terminal YFP fusion does not interfere with 14-3-3-ligand interactions.

14-3-3σ and 14-3-3ζ have a different subcellular distribution

To study the subcellular distribution of 14-3-3 isoforms we transiently transfected various mammalian cell types and determined the localisation of 14-3-3σ-YFP and 14-3-3ζ-YFP.

Control experiments, in which transfected and untransfected cells were immunostained, showed that transfection had no effect on the distribution of endogenous 14-3-3σ and 14-3-3ζ (data not shown). In all cell types investigated, 14-3-3σ had a mainly diffuse cytoplasmic distribution and only low levels of fluorescence were observed in the nucleus (Fig. 3A, left panel). The intracellular distribution of 14-3-3ζ-YFP was clearly different. A diffuse cytoplasmic and nuclear localisation was observed, although fluorescence in the nucleus was slightly lower than in the cytoplasm (Fig. 3A, right panel). Nuclear (F_N) and cytoplasmic (F_C) 14-3-3 levels were determined and the ratio F_N/F_C was calculated for each cell type (Fig. 3B). 14-3-3σ and 14-3-3ζ had a clearly distinct intracellular distribution in all cell types investigated. The F_N/F_C ratio of 14-3-3ζ was about twice that of 14-3-3σ. Immunolocalisation of endogenous 14-3-3σ and 14-3-3ζ with specific antibodies in HaCaT and Hela cells revealed similar subcellular distributions as were found with the 14-3-3-YFP constructs (Fig. 3B; Fig. 3C, hatched bars). This indicates that results obtained with YFP-labelled 14-3-3 isoforms have biological significance.

We further investigated the subcellular distribution of 14-3-3 by biochemical fractionation of HaCaT cells into a cytosolic and nuclear extract. Equal amounts of total protein from both extracts were analysed by western blotting with specific antibodies for 14-3-3σ (Fig. 4A) and 14-3-3ζ (Fig. 4B). 14-3-3σ appears to be mainly cytosolic, although a small amount can be seen in the nucleus (not visible in this exposure) when more protein is loaded (data not shown). The majority of 14-3-3ζ is cytosolic, but a significant amount is present in the nucleus (Fig. 4B). A control experiment with antibodies against known nuclear (p53), cytoplasmic (RasGAP, PKCζ) and cytoskeletal
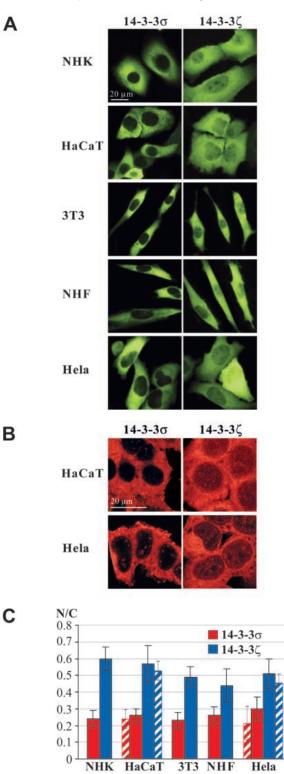

Fig. 3. (A) Subcellular distribution of 14-3-3σ-YFP and 14-3-3ζ-YFP in the indicated mammalian cells. (B) HaCaT and Hela cells immunostained for endogenous 14-3-3σ and 14-3-3ζ. (C) Quantitative analysis of the subcellular distribution of 14-3-3σ (red) and 14-3-3ζ (blue). Solid bars represent the average nuclear/cytoplasmic (F_N/F_C) ratio obtained with YFP-labelled 14-3-3 isoforms. Hatched bars represent the quantitative analysis of immunolocalisations of endogenous 14-3-3σ and ζ. Standard deviations are indicated (black lines).

(actin, α-tubulin) proteins shows that the nuclear extract is not contaminated with cytoplasmic or cytoskeletal proteins and that the cytosolic fraction is not contaminated with nuclear proteins (Fig. 4C). These data confirm the results from microscopic analysis.
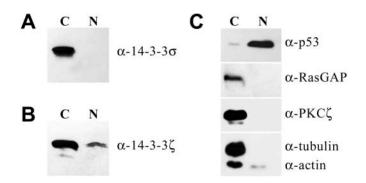

Fig. 4. Subcellular distribution of 14-3-3 after biochemical cell fractionation. HaCaT cells were fractionated into a cytosolic (C) and nuclear extract (N). Equal amounts of total protein from both extracts were analysed by western blotting. (A) Blot stained with specific 14-3-3σ antibodies or (B) specific 14-3-3ζ antibodies. (C) Control probed with antibodies against known nuclear (p53), cytoplasmic (RasGAP, PKCζ) and cytoskeletal (actin, α-tubulin) proteins.

Crm1-dependent export of 14-3-3σ and 14-3-3ζ

Both 14-3-3σ and 14-3-3ζ contain a putative nuclear export sequence (NES). Therefore, we studied the effect of the Crm1-dependent nuclear export inhibitor LMB on the intracellular 14-3-3 distribution. Treatment of HaCaT cells expressing 14-3-3σ-YFP with LMB led to a clear increase in nuclear 14-3-3σ concentration (Fig. 5A). For 14-3-3ζ, a similar increase in nuclear concentration was observed, although the effect appeared to be less strong. The nuclear accumulation of 14-3-3σ and 14-3-3ζ had already reached its maximum 2 hours after LMB treatment and no significant changes were observed 4, 5 and 24 hours after the addition of LMB. A fraction of cells appeared relatively unresponsive to LMB treatment. We calculated the F_N/F_C ratio for 50 HaCaT cells expressing either 14-3-3σ-YFP or 14-3-3ζ-YFP, with and without LMB treatment (Fig. 5B). Untreated cells expressing 14-3-3σ-YFP had an average F_N/F_C of 0.31±0.07. Subsequently, the percentage of cells with an F_N/F_C ratio higher than 0.45 (average F_N/F_C plus two times standard deviation of untreated cells) was calculated (Fig. 5C). Untreated cells expressing 14-3-3ζ-YFP had an average F_N/F_C of 0.59±0.09, and therefore we calculated the percentage of cells with F_N/F_C>0.77 for 14-3-3ζ (Fig. 5C).

To study the effect of LMB treatment on the subcellular distribution of endogenous 14-3-3 proteins, we immunostained
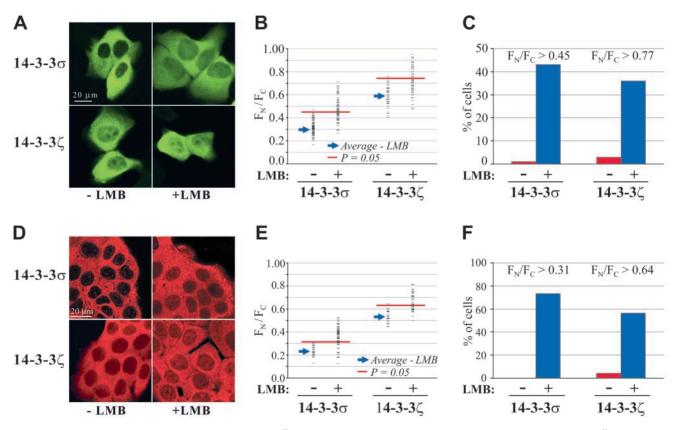

Fig. 5. Effect of LMB on intracellular 14-3-3σ and 14-3-3ζ distribution. (A) HaCaT cells expressing 14-3-3σ-YFP or 14-3-3ζ-YFP were incubated in medium with or without LMB for 5 hours. (B) Plot of the individual F_N/F_C ratios for 14-3-3σ-YFP and 14-3-3ζ-YFP of 50 cells, with and without LMB treatment. (C) Percentage of cells with a significantly increased F_N/F_C ratio (F_N/F_C>0.45 for 14-3-3σ and F_N/F_C>0.77 for 14-3-3ζ). (D) HaCaT cells incubated in medium with or without LMB for 5 hours were immunostained with specific antibodies for 14-3-3σ or 14-3-3ζ. (E) Plot of the individual F_N/F_C ratios for endogenous 14-3-3σ and 14-3-3ζ of cells treated with and without LMB. (F) Percentage of cells with a significantly increased F_N/F_C ratio of endogenous 14-3-3 (F_N/F_C>0.31 for 14-3-3σ and F_N/F_C>0.64 for 14-3-3ζ).

untreated and LMB-treated HaCaT cells with antibodies specific for 14-3-3σ or 14-3-3ζ (Fig. 5D). LMB treatment led to a noticeable increase in nuclear 14-3-3 concentration. As described above, we determined the F_N/F_C ratio for individual cells immunostained for either 14-3-3σ or 14-3-3ζ, with and without LMB treatment (Fig. 5E). Subsequently, the percentage of cells with an F_N/F_C ratio higher than 0.31 for 14-3-3σ and higher than 0.64 for 14-3-3ζ was calculated (Fig. 5F). As was found with the YFP-labelled isoforms, LMB treatment appeared to have a stronger effect on the nuclear accumulation of 14-3-3σ than that of 14-3-3ζ.

Our data show that LMB treatment leads to a significant increase in nuclear 14-3-3 levels, indicating that 14-3-3 is exported at least in part by a NES- and Crm1-dependent mechanism. The fact that LMB treatment leads to a significant, but not complete accumulation of 14-3-3 in the nucleus, suggests that, besides Crm1-dependent export, other export mechanisms are also involved. A fivefold higher LMB concentration did not result in increased nuclear accumulation (data not shown), which is in line with the findings of others that the LMB concentrations used in this study are sufficient to give an almost complete inhibition of Crm1.

Nuclear import and export rates of 14-3-3σ and 14-3-3ζ

Why do 14-3-3σ and 14-3-3ζ have a different subcellular distribution? 14-3-3σ is either imported more slowly or exported more rapidly than 14-3-3ζ. To investigate this aspect, we studied the nuclear import and export of 14-3-3σ and 14-3-3ζ using FRAP in the presence and absence of LMB. A region covering >75% of the nucleus of HaCaT cells expressing 14-3-3σ-YFP, 14-3-3ζ-YFP or YFP alone was photobleached for 3 seconds, after which fluorescence recovery in the nucleus was followed over time (Fig. 6A). Photobleaching a square region in the nucleus for 3 seconds did not lead to a discrete square photobleached zone, but resulted in a homogenous decrease in fluorescence throughout the entire nucleus (Fig. 6A). This shows that the 14-3-3 proteins are highly mobile within the nucleoplasm and therefore that the observed relatively slow fluorescence recovery in the nucleus is the result of exchange of photobleached molecules for fluorescent molecules from the cytoplasm. Time-dependent recovery of nuclear fluorescence was quantified and the nuclear import (k_i) and export (k_e) rate constants and half-times ($\tau_{1/2}$) were determined as described in Materials and Methods. Repeated photobleaching of the nucleus of the same cell yielded similar half-times (data not shown), indicating that the photobleaching process did not affect the import-export process. Typical normalised recovery curves for 14-3-3σ-YFP, 14-3-3ζ-YFP and the YFP control are shown in Fig. 6B. A $\tau_{1/2}$ of 5.7±1.5 seconds and 9.7±1.5 seconds was found for the nuclear export of 14-3-3σ-YFP and 14-3-3ζ-YFP, respectively. For nuclear import, a $\tau_{1/2}$ of 18 seconds was found for both 14-3-3σ-YFP and 14-3-3ζ-YFP. As the k_e of 14-3-3σ is 1.7 times higher than the k_e of 14-3-3ζ, while the k_is are equal, the different subcellular distribution of 14-3-3σ compared with 14-3-3ζ appears to be caused by the more efficient export of 14-3-3σ. Comparing these values to the $\tau_{1/2}$ of 61±15 seconds for the passive diffusion of YFP alone suggests that the 14-3-3 proteins shuttle rapidly in and out of the nucleus through active transport. To ensure that the
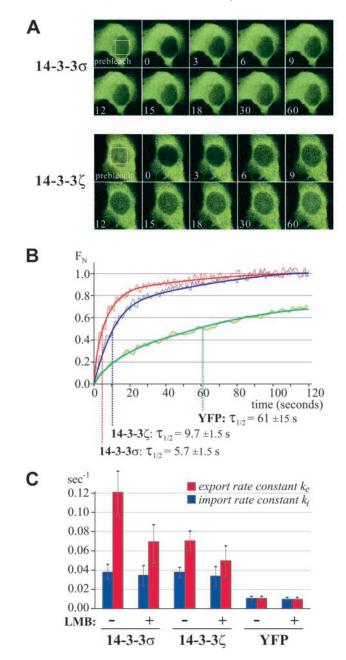

Fig. 6. FRAP analysis of nucleocytoplasmic transport of 14-3-3 proteins. (A) A region covering >75% of the nucleus (indicated by the white box) of HaCaT cells expressing 14-3-3σ-YFP or 14-3-3ζ-YFP was photobleached, after which images were recorded at 1-second intervals. Fluorescence recovery is shown for two representative cells at the indicated times in seconds. (B) Typical normalised recovery curves with $\tau_{1/2}$ for nuclear export for 14-3-3σ-YFP, 14-3-3ζ-YFP and YFP alone. (C) Rate constants for the nuclear import and export of 14-3-3σ-YFP, 14-3-3ζ-YFP and YFP alone, in untreated and LMB-treated cells. At least 15 cells were measured and quantified in each experiment.

results from our FRAP experiments reflect nuclear export of 14-3-3, we performed FRAP experiments on cells treated with the nuclear export inhibitor LMB. Fig. 6C shows the k_is and k_es for 14-3-3σ-YFP, 14-3-3ζ-YFP and YFP alone in untreated and LMB-treated cells. LMB treatment reduced the k_e for

14-3-3σ export by 45% and by 30% for 14-3-3ζ (Fig. 6C). The k_is (calculated from the k_e and the increased F_N/F_C) were not significantly reduced after LMB treatment. This suggests that 14-3-3σ and, to a lesser extent, 14-3-3ζ are exported at least in part by a Crm1-dependent mechanism.

Discussion

Nucleocytoplasmic transport of proteins plays an important role in the regulation of many cellular processes. Differences in the kinetics of nuclear shuttling can provide a basis for isoform-specific functional specialisation of members of multigene families. This is particularly significant for conserved protein families, like the 14-3-3 proteins. Many organisms contain multiple 14-3-3 isoforms and, thus far, it remains unclear whether and to what extent these isoforms have specialised biological functions and whether these are based on temporal and tissue-specific expression regulation and/or on isoform-specific ligand binding. In addition, ambiguous and conflicting data have been reported on the specific subcellular distribution of isoforms (Roth et al., 1994; Martin et al., 1994; Sehnke et al., 2000; Pietromonaco et al., 1996). To gain more insight in this matter, we studied the subcellular distribution and dynamic localisation of 14-3-3σ and 14-3-3ζ in living mammalian cells.

We first showed that recombinant human 14-3-3-YFP constructs are functional in vivo in yeast, that they form dimers in vitro and are able to bind a Raf-1-based peptide. This suggests that the fusion of YFP to the C-terminus and a 6×His-tag to the N-terminus of 14-3-3 does not interfere with the major 14-3-3 functions.

The subcellular distribution of 14-3-3σ and 14-3-3ζ was studied in various mammalian cell types by immunostaining endogenous 14-3-3 proteins with specific antibodies and by analysis of cells transiently expressing YFP fusions of these proteins. Biochemical fractionation of HaCaT cells provided additional insight in the isoform-specific subcellular distribution of the 14-3-3 proteins. 14-3-3σ exhibited a mainly diffuse cytoplasmic distribution and was present at low levels in the nucleus. But nuclear concentrations of 14-3-3ζ-YFP were noticeably higher in comparison with 14-3-3σ. F_N/F_C ratios of 0.26 and 0.52 were found for 14-3-3σ and 14-3-3ζ, respectively. No significant differences in subcellular distribution were found between the various cell types, indicating that the mechanism responsible for the more efficient nuclear exclusion of 14-3-3σ is unlikely to be cell-type specific, as it is even present in cell types that normally do not express 14-3-3σ (e.g. NIH-3T3 and NHF).

We performed FRAP experiments on living cells to study the mechanism underlying the different subcellular distributions of 14-3-3σ and 14-3-3ζ. Both 14-3-3σ and 14-3-3ζ rapidly shuttle in and out of the nucleus through active transport. 14-3-3σ had a 1.7× higher nuclear export rate constant than 14-3-3ζ, whereas import rate constants were equal. Therefore, the difference in subcellular distribution between 14-3-3σ and 14-3-3ζ appeared to be caused by the more efficient export of 14-3-3σ. Treatment of cells with LMB led to an increase in nuclear 14-3-3 levels and to a significant decrease of the export rate constants of both 14-3-3σ and 14-3-3ζ, suggesting that these proteins are exported at least in part by a Crm1-dependent mechanism.

One possible explanation for the different subcellular distributions and export rates of 14-3-3σ and 14-3-3ζ might rely on the finding that nuclear export of 14-3-3 could be governed by binding partners. In this model, 14-3-3 itself plays no active role in nuclear export and is exported out of the nucleus via a 'piggy-back' mechanism in which the binding partner provides the NES (Brunet et al., 2002). Isoform-specific ligand interactions would in this case cause the different subcellular distributions of 14-3-3σ and 14-3-3ζ. 14-3-3σ might preferentially bind ligands that are rapidly exported from the nucleus. This model, however, does not explain why 14-3-3 is required for the nuclear export of some binding partners (Wang and Yang, 2001; Brunet et al., 2002).

An alternative model is that sequences in 14-3-3 itself govern nuclear export. It has been reported that a putative NES is present in the C-terminus of 14-3-3, in a region that also appeared to be involved in ligand binding (Lopez et al., 1999; Rittinger et al., 1999). Although this sequence was able to function as NES when fused to GFP, a recent study suggests that this region is only involved in ligand binding (Brunet et al., 2002). However, one could envisage that the NES of 14-3-3 is (partly) folded into the ligand-binding groove in the absence of a binding partner, leading to nuclear retention of unbound 14-3-3. In support of this, the C-terminus appears to function in the inhibition of improper 14-3-3-ligand interactions by occupying the ligand binding groove (Truong et al., 2002). On ligand binding, the NES might be displaced from the groove and become exposed, leading to nuclear export through Crm1. In such a model, unbound 14-3-3 would home to the nucleus, where after ligand binding its NES is exposed, leading to rapid translocation to the cytoplasm. This model would explain why 14-3-3 is required for the nuclear export of certain ligands (Brunet et al., 2002). As 14-3-3σ and 14-3-3ζ both contain an identical NES consensus motif (216-DLIMQLLRDNLTLW) in their C-termini, it is unlikely that this region is responsible for the difference in subcellular distribution of these isoforms. However, the extreme C-terminal region directly flanking the putative NES, which might be involved in the structural changes mentioned above, is highly divergent and could account for the observed isoform specificity. Clearly, more experiments, which are beyond the focus of this analysis, are needed to elucidate the molecular mechanisms that underlie the isoform-specific export rates that we have measured.

In conclusion, we have shown differences in the subcellular distribution and nuclear export kinetics of 14-3-3 proteins, which might be the basis for isoform-specific biological functions. Our data indicate that one should not think of the 14-3-3 proteins as static molecules that passively sequester ligands in the cytoplasm. On the contrary, 14-3-3 proteins rapidly shuttle in and out of the nucleus, making fast responses to signals possible and allowing them to play an active role in changing the localisation of binding partners. The rapid nuclear export of 14-3-3σ in particular is interesting, as it might reflect a mechanism by which cells can efficiently control the nuclear exclusion of proteins involved in cell cycle progression. The high export rates of 14-3-3σ are in line with a transient function of this protein in the nucleus and with the proposed role of 14-3-3σ in causing rapid DNA damage-induced cell cycle arrest through its p53-mediated upregulation and cytoplasmic sequestering of Cdc2 (Laronga et al., 2000; Chan et al., 1999; Hermeking et al., 1997). The fact that YFP fusion constructs

are functional and have the same subcellular distribution as endogenous 14-3-3 isoforms creates new and interesting possibilities for future functional studies on 14-3-3 proteins in living cells. Our findings might reflect a mechanism that can be the basis for isoform-specific specialisations within multigene families in general.

References

Brunet, A., Kanai, F., Stehn, J., Xu, J., Sarbassova, D., Frangioni, J. V., Dalal, S. N., DeCaprio, J. A., Greenberg, M. E. and Yaffe, M. B. (2002). 14-3-3 transits to the nucleus and participates in dynamic nucleocytoplasmic transport. *J. Cell Biol.* **156**, 817-828.

Chan, T. A., Hermeking, H., Lengauer, C., Kinzler, K. W. and Vogelstein, B. (1999). 14-3-3Sigma is required to prevent mitotic catastrophe after DNA damage. *Nature* **401**, 616-620.

Chen, Z., Fu, H., Liu, D., Chang, P. F., Narasimhan, M., Ferl, R., Hasegawa, P. M. and Bressan, R. A. (1994). A NaCl-regulated plant gene encoding a brain protein homology that activates ADP ribosyltransferase and inhibits protein kinase C. *Plant J.* **6**, 729-740.

Craparo, A., Freund, R. and Gustafson, T. A. (1997). 14-3-3 epsilon interacts with the insulin-like growth factor I receptor and insulin receptor substrate I in a phosphoserine-dependent manner. *J. Biol. Chem.* **272**, 11663-11669.

Dalal, S. N., Schweitzer, C. M., Gan, J. M. and DeCaprio, J. A. (1999). Cytoplasmic localization of human cdc25C during interphase requires an intact 14-3-3 binding site. *Mol. Cell. Biol.* **19**, 4465-4479.

de Vetten, N. C. and Ferl, R. J. (1995). Characterization of a maize G-box binding factor that is induced by hypoxia. *Plant J.* **7**, 589-601.

Fanger, G. R., Widmann, C., Porter, A. C., Sather, S., Johnson, G. L. and Vaillancourt, R. R. (1998). 14-3-3 proteins interact with specific MEK kinases. *J. Biol. Chem.* **273**, 3476-3483.

Garcia, G. M., Dolfi, F., Russello, M. and Vuori, K. (1999). Cell adhesion regulates the interaction between the docking protein p130(Cas) and the 14-3-3 proteins. *J. Biol. Chem.* **274**, 5762-5768.

Gietz, R. D., Schiestl, R. H., Willems, A. R. and Woods, R. A. (1995). Studies on the transformation of intact yeast cells by the LiAc/SS-DNA/PEG procedure. *Yeast* **11**, 355-360.

Gietz, R. D. and Sugino, A. (1988). New yeast-Escherichia coli shuttle vectors constructed with in vitro mutagenized yeast genes lacking six-base pair restriction sites. *Gene* **74**, 527-534.

Hashiguchi, M., Sobue, K. and Paudel, H. K. (2000). 14-3-3z is an affector of Tau protein phosphorylation. *J. Biol. Chem.* **275**, 25247-25254.

Hermeking, H., Lengauer, C., Polyak, K., He, T. C., Zhang, L., Thiagalingam, S., Kinzler, K. W. and Vogelstein, B. (1997). 14-3-3 sigma is a p53-regulated inhibitor of G2/M progression. *Mol. Cell.* **1**, 3-11.

Iwata, N., Yamamoto, H., Sasaki, S., Itoh, F., Suzuki, H., Kikuchi, T., Kaneto, H., Iku, S., Ozeki, I., Karino, Y. et al. (2000). Frequent hypermethylation of CpG islands and loss of expression of the 14-3-3 sigma gene in human hepatocellular carcinoma. *Oncogene* **19**, 5298-5302.

Jarillo, J. A., Capel, J., Leyva, A., Martinez-Zapater, J. M. and Salinas, J. (1994). Two related low-temperature-inducible genes of Arabidopsis encode proteins showing high homology to 14-3-3 proteins, a family of putative kinase regulators. *Plant Mol. Biol.* **25**, 693-704.

Jones, D. H. A., Martin, H., Madrazo, J., Robinson, K. A., Nielsen, P., Roseboom, P. H., Patel, Y., Howell, S. A. and Aitken, A. (1995). Expression and structural analysis of 14-3-3 proteins. *J. Mol. Biol.* **245**, 375-384.

Kidou, S., Umeda, M., Kato, A. and Uchimiya, H. (1993). Isolation and characterization of a rice cDNA similar to the bovine brain-specific 14-3-3 protein gene. *Plant Mol. Biol.* **21**, 191-194.

Ku, N. O., Liao, J. and Omary, M. B. (1998). Phosphorylation of human keratin 18 serine 33 regulates binding to 14-3-3 proteins. *EMBO J.* **17**, 1892-1906.

Kumagai, A. and Dunphy, W. G. (1999). Binding of 14-3-3 proteins and nuclear export control the intracellular localization of the mitotic inducer Cdc25. *Genes Dev.* **13**, 1067-1072.

Kumagai, A., Yakowec, P. S. and Dunphy, W. G. (1998). 14-3-3 proteins act as negative regulators of the mitotic inducer Cdc25 in Xenopus egg extracts. *Mol. Biol. Cell* **9**, 345-354.

Kurz, E. U., Leader, K. B., Kroll, D. J., Clark, M. and Gieseler, F. (2000). Modulation of human DNA topoisomerase IIalpha function by interaction with 14-3-3 epsilon. *J. Biol. Chem.* **275**, 13948-13954.

Laronga, C., Yang, H. Y., Neal, C. and Lee, M. H. (2000). Association of the cyclin-dependent kinases and 14-3-3 sigma negatively regulates cell cycle progression. *J. Biol. Chem.* **275**, 23106-23112.

Leffers, H., Madsen, P., Rasmussen, H. H., Honore, B., Andersen, A. H., Walbum, E., Vandekerckhove, J. and Celis, J. E. (1993). Molecular cloning and expression of the transformation sensitive epithelial marker stratifin. A member of a protein family that has been involved in the protein kinase C signalling pathway. *J. Mol. Biol.* **231**, 982-998.

Lennon, G., Auffray, C., Polymeropoulos, M. and Soares, M. B. (1996). The I.M.A.G.E. Consortium: an integrated molecular analysis of genomes and their expression. *Genomics* **33**, 151-152.

Liu, Y. C., Liu, Y., Elly, C., Yoshida, H., Lipkowitz, S. and Altman, A. (1997). Serine phosphorylation of Cbl induced by phorbol ester enhances its association with 14-3-3 proteins in T cells via a novel serine-rich 14-3-3-binding motif. *J. Biol. Chem.* **272**, 9979-9985.

Lopez, G. A., Furnari, B., Mondesert, O. and Russell, P. (1999). Nuclear localization of Cdc25 is regulated by DNA damage and a 14-3-3 protein. *Nature* **397**, 172-175.

Marenholz, I., Zirra, M., Fischer, D. F., Backendorf, C., Ziegler, A. and Mischke, D. (2001). Identification of human epidermal differentiation complex (EDC)-encoded genes by subtractive hybridization of entire YACs to a gridded keratinocyte cDNA library. *Genome Res.* **11**, 341-355.

Markiewicz, E., Wiczynski, G., Rzepecki, R., Kulma, A. and Szopa, J. (1996). The 14-3-3 protein binds to the nuclear matrix endonuclease and has a possible function in the control of plant senescence. *Cell Mol. Biol. Lett.* **1**, 391-415.

Martin, H., Rostas, J., Patel, Y. and Aitken, A. (1994). Subcellular localisation of 14-3-3 isoforms in rat brain using specific antibodies. *J. Neurochem.* **63**, 2259-2265.

Meller, N., Liu, Y. C., Collins, T. L., BonnefoyBerard, N., Baier, G., Isakov, N. and Altman, A. (1996). Direct interaction between protein kinase C theta (PKC theta) and 14-3-3 tau in T cells: 14-3-3 overexpression results in inhibition of PKC theta translocation and function. *Mol. Cell. Biol.* **16**, 5782-5791.

Muslin, A. J., Tanner, J. W., Allen, P. M. and Shaw, A. S. (1996). Interaction of 14-3-3 with signaling proteins is mediated by the recognition of phosphoserine. *Cell* **84**, 889-897.

Pellegrini, G., Dellambra, E., Golisano, O., Martinelli, E., Fantozzi, I., Bondanza, S., Ponzin, D., McKeon, F. and de Luca, M. (2001). p63 identifies keratinocyte stem cells. *Proc. Natl. Acad. Sci. USA* **98**, 3156-3161.

Peng, C. Y., Graves, P. R., Thoma, R. S., Wu, Z., Shaw, A. S. and Piwnica, W. H. (1997). Mitotic and G2 checkpoint control: regulation of 14-3-3 protein binding by phosphorylation of Cdc25C on serine-216. *Science* **277**, 1501-1505.

Perego, L. and Berruti, G. (1997). Molecular cloning and tissue-specific expression of the mouse homologue of the rat brain 14-3-3 theta protein: characterization of its cellular and developmental pattern of expression in the male germ line. *Mol. Reprod. Dev.* **47**, 370-379.

Petosa, C., Masters, S. C., Bankston, L. A., Pohl, J., Wang, B. C., Fu, H. I. and Liddington, R. C. (1998). 14-3-3 zeta binds a phosphorylated Raf peptide and an unphosphorylated peptide via its conserved amphipathic groove. *J. Biol. Chem.* **273**, 16305-16310.

Pietromonaco, S. F., Seluja, G. A., Aitken, A. and Elias, L. (1996). Association of 14-3-3 proteins with centrosomes. *Blood Cells Mol. Dis.* **22**, 225-237.

Rittinger, K., Budman, J., Xu, J., Volinia, S., Cantley, L. C., Smerdon, S. J., Gamblin, S. J. and Yaffe, M. B. (1999). Structural analysis of 14-3-3 phosphopeptide complexes identifies a dual role for the nuclear export signal of 14-3-3 in ligand binding. *Mol. Cell* **4**, 153-166.

Roth, D. and Burgoyne, R. D. (1995). Stimulation of catecholamine secretion from adrenal chromaffin cells by 14-3-3 proteins is due to reorganisation of the cortical actin network. *FEBS Lett.* **374**, 77-81.

Roth, D., Morgan, A., Martin, H., Jones, D., Martens, G. J., Aitken, A. and Burgoyne, R. D. (1994). Characterization of 14-3-3 proteins in adrenal chromaffin cells and demonstration of isoform-specific phospholipid binding. *Biochem. J.* **301**, 305-310.

Sark, M. W., Fischer, D. F., de Meijer, E., van de Putte, P. and Backendorf, C. (1998). AP-1 and ets transcription factors regulate the expression of the human SPRR1A keratinocyte terminal differentiation marker. *J. Biol. Chem.* **273**, 24683-24692.

Sehnke, P. C., Henry, R., Cline, K. and Ferl, R. J. (2000). Interaction of a plant 14-3-3 protein with the signal peptide of a thylakoid-targeted chloroplast precursor protein and the presence of 14-3-3 isoforms in the chloroplast stroma. *Plant Physiol.* **122**, 235-242.

Subramanian, R. R., Masters, S. C., Zhang, H. and Fu, H. (2001). Functional conservation of 14-3-3 isoforms in inhibiting bad-induced apoptosis. *Exp. Cell Res.* **271**, 142-151.

Tang, S. J., Suen, T. C., McInnes, R. R. and Buchwald, M. (1998). Association of the TLX-2 homeodomain and 14-3-3eta signaling proteins. *J. Biol. Chem.* **273**, 25356-25363.

Tien, A. C., Hsei, H. Y. and Chien, C. T. (1999). Dynamic expression and cellular localization of the drosophila 14-3-3 epsilon during embryonic development. *Mech. Dev.* **81**, 209-212.

Todd, A., Cossons, N., Aitken, A., Price, G. B. and Zannis-Hadjopoulos, M. (1998). Human cruciform binding protein belongs to the 14-3-3 family. *Biochemistry* **37**, 14317-14325.

Truong, A. B., Masters, S. C., Yang, H. and Fu, H. (2002). Role of the 14-3-3 C-terminal loop in ligand interaction. *Proteins* **49**, 321-325.

Tzivion, G. and Avruch, J. (2002). 14-3-3 proteins: active cofactors in cellular regulation by serine/threonine phosphorylation. *J. Biol. Chem.* **277**, 3061-3064.

Van Der Hoeven, P. C., van Der Wal, J. C., Ruurs, P., van Dijk, M. C. and van Blitterswijk, J. (2000). 14-3-3 isotypes facilitate coupling of protein kinase C-zeta to Raf-1: negative regulation by 14-3-3 phosphorylation. *Biochem. J.* **345**, 297-306.

van Hemert, M. J., Steensma, H. Y. and van Heusden, G. P. (2001). 14-3-3 proteins: key regulators of cell division, signalling and apoptosis. *Bioessays* **23**, 936-946.

van Heusden, G. P. H., Griffiths, D. J., Ford, J. C., Chin, A. W.-T., Schrader, P. A., Carr, A. M. and Steensma, H. Y. (1995). The 14-3-3 proteins encoded by the BMH1 and BMH2 genes are essential in the yeast Saccharomyces cerevisiae and can be replaced by a plant homologue. *Eur. J. Biochem.* **229**, 45-53.

van Heusden, G. P. H., van-der-Zanden, A. L., Ferl, R. J. and Steensma, H. Y. (1996). Four Arabidopsis thaliana 14-3-3 protein isoforms can complement the lethal yeast bmh1 bmh2 double disruption. *FEBS Lett.* **391**, 252-256.

van Zeijl, M. J., Testerink, C., Kijne, J. W. and Wanga, M. (2000). Subcellular differences in post-translational modification of barley 14-3-3 proteins. *FEBS Lett.* **473**, 292-296.

Wakui, H., Wright, A. P., Gustafsson, J. and Zilliacus, J. (1997). Interaction of the ligand-activated glucocorticoid receptor with the 14-3-3 eta protein. *J. Biol. Chem.* **272**, 8153-8156.

Wang, A. H. and Yang, X. J. (2001). Histone deacetylase 4 possesses intrinsic nuclear import and export signals. *Mol. Cell. Biol.* **21**, 5992-6005.

Yaffe, M. B. (2002). How do 14-3-3 proteins work? Gatekeeper phosphorylation and the molecular anvil hypothesis. *FEBS Lett.* **513**, 53-57.

Zhang, S. H., Kobayashi, R., Graves, P. R., Piwnica-Worms, H. and Tonks, N. K. (1997). Serine phosphorylation-dependent association of the band 4.1-related protein-tyrosine phosphatase PTPH1 with 14-3-3beta protein. *J. Biol. Chem.* **272**, 27281-27287.

Zonneveld, B. J. M. (1986). Cheap and simple yeast media. *J. Microbiol. Methods* **4**, 287-291.